

AN APPRAISAL OF PEAK TEMPERATURES AND THERMAL HISTORIES IN ULTRAHIGH-TEMPERATURE (UHT) CRUSTAL METAMORPHISM: THE SIGNIFICANCE OF ALUMINOUS ORTHOPYROXENE

Simon L. HARLEY

*Department of Geology and Geophysics, University of Edinburgh,
Kings Buildings, West Mains Road, Edinburgh,
Scotland EH9 3JW, U.K.*

Abstract: Ultrahigh-temperature (UHT) crustal metamorphism occurs where peak metamorphic temperatures of 900–1100°C have been attained at pressures in the range 7–13 kbar. Mineral assemblages in metapelites that are constrained by experimentally-derived and calculated FMAS and KFMASH petrogenetic grids provide good evidence for UHT conditions. Sapphirine+quartz is stable only at >1040°C in reduced rocks, and orthopyroxene+sillimanite+quartz is restricted to pressures greater than 8 kbar at $T > 900^\circ\text{C}$ in KFMASH. New Fe-Mg exchange thermometry and thermometry based on Al in orthopyroxene coexisting with garnet allows a re-evaluation of the peak or near-peak temperatures in UHT terrains. The J. GANGULY *et al.* (Contrib. Mineral. Petrol., **126**, 137, 1996) garnet-orthopyroxene Fe-Mg thermometer yields temperature estimates in the range 900–1100°C for several UHT case studies, but closes at lower temperatures in other cases. Thermometry based on the high Al₂O₃ contents (8–12 wt%) of orthopyroxene coexisting with garnet, in sillimanite- and sapphirine-bearing assemblages that are constrained from the grids to be >1000°C, support the UHT nature of the areas for which reliable data are available. For example, the FAS-system orthopyroxene Al-geothermometer (L.Y. ARANOVICH and R.G. BERMAN, Am. Mineral., **82**, 345, 1997) yields average temperature estimates of $962 \pm 51^\circ\text{C}$ for granulites from the Napier Complex, Rauer Islands, Sri Lanka, Eastern Ghats and similar UHT areas.

Elemental mapping of Al zoning in orthopyroxene coexisting with garnet or other aluminous phases can provide insight into pre- and post-peak thermal histories of UHT terrains. In the Napier Complex orthopyroxene coexisting with sapphirine+quartz zones from over 12 wt% Al₂O₃ in cores down to only ca. 9 wt% Al₂O₃ in rims and recrystallised grains. This zoning reflects cooling through 80°C within the stability field of sapphirine + quartz, and leads to a new estimate of $1120 \pm 20^\circ\text{C}$ for the peak temperature of regional metamorphism in this UHT terrain. At Mather Peninsula in the Rauer Islands early orthopyroxenes that have grown with porphyroblastic garnet are zoned from cores with only ca. 8 wt% Al₂O₃ to rims with up to 10.5 wt% Al₂O₃. This zoning may reflect prograde heating of $90 \pm 20^\circ\text{C}$ through the interval 950–1050°C at 9–12 kbar, corresponding to the temperature interval over which melts are generated in and segregated from these gneisses. The formation and local segregation of water-undersaturated melts is likely to be fundamental to both the generation and preservation of the record of UHT metamorphic histories.

key words: metamorphism, granulite, ultrahigh temperature, geothermometry, orthopyroxene, mineral chemical zoning.

mineral abbreviations: Bt-biotite; Crd-cordierite; Grt-garnet; Kfs-K feldspar; Ky-kyanite; L-liquid (granitic melt); Opx-orthopyroxene; Os-osumilite; Plag-plagioclase; Qz-quartz; Sil-sillimanite; Spl-spinel; Spr-sapphire.

1. Introduction

In recent years what we now regard as being the pressure-temperature domain of metamorphism has been vastly expanded as the extremes of metamorphism have become more clearly documented in the geological record. With respect to extremes of temperature, the significance of ultra high temperature (UHT) regional metamorphism in which crustal rocks are subjected to temperatures of 900–1100°C at only moderate pressures (7–13 kbar) is now widely recognised (HARLEY, 1998a). Indeed, it has become apparent that an understanding of the pressure-temperature (P - T) conditions and P - T histories of such granulites is central to any tectonomagmatic models applied to high-grade gneiss terranes and more broadly to the behaviour of continental crust in collision and extension (e.g. BOHLEN, 1991; ELLIS, 1987; HARLEY, 1989; SANDIFORD and POWELL, 1991).

HARLEY (1998a) has recently presented an overview of UHT crustal metamorphism that includes descriptions of important examples, an evaluation of some of the mineral assemblage and thermobarometric constraints relevant to UHT conditions, and a description and appraisal of the application of reaction textures to constraining post-peak IBC and ITD histories. In that study (HARLEY, 1998a) it was emphasised that the available cation-partitioning geothermometry is often at odds with assemblage constraints, so that reliable estimation of peak temperatures remains an important problem in UHT metamorphism. In the short time since that study was written two new calibrations of thermometers applicable to UHT garnet-orthopyroxene assemblages have appeared (GANGULY *et al.*, 1996; ARANOVICH and BERMAN, 1997) that permit further evaluation of the temperature field of UHT metamorphism and also enable further consideration of the significance of Al and Fe-Mg zoning relationships. This work firstly examines the applicability of the recent geothermometers to UHT terrains, and compares the results of peak-T estimates obtained using these calibrations with those derived from the Al-thermometer based on HARLEY and GREEN (1982). Secondly, Al₂O₃ zoning patterns in orthopyroxenes are used to interpret the thermal histories and peak temperatures of the Napier Complex and Rauer Islands and to demonstrate the potential of elemental mapping and other imaging techniques for yielding further insights into UHT crustal metamorphism.

2. The P - T Field of UHT Metamorphism and the Principal Assemblage Constraints

UHT metamorphism forms a sub-division of the granulite facies (3–15 kbar and 700–1000°C: HARLEY, 1989), and is defined as crustal metamorphism that has occurred at peak conditions of greater than 900°C and at mid- to deep-crustal levels equivalent to pressures in the range 7–13 kbar. This definition effectively excludes high- T /low- P terrains from the field of UHT as the maximum temperatures attained in these seldom exceed 850°C, even at depths equivalent to 5–6 kbar (WATERS, 1991). The rationale for this definition lies in

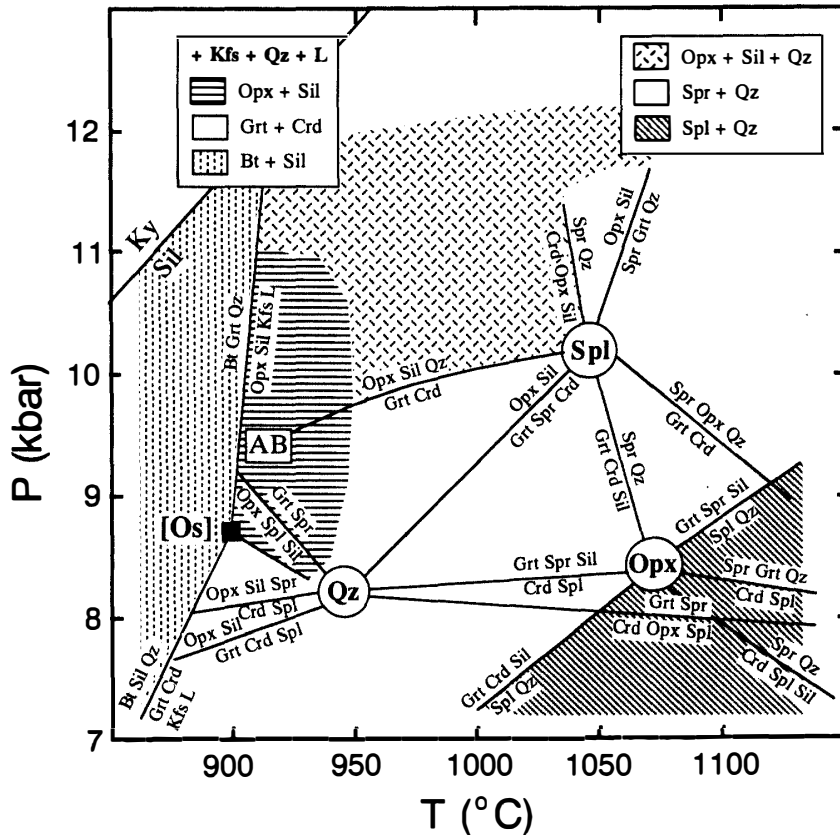


Fig. 1. *P-T* diagram of mineral assemblage constraints on UHT assemblages. The model FMAS-system grid for low f_{O_2} pelites is modified after HENSEN and GREEN (1973) and BERTRAND *et al.* (1991). Part of the KFMASH system, featuring reactions between Bt, Grt, Sil, Crd, Opx, Os, Qz, Kfs and L (CARRINGTON and HARLEY, 1995a; HOLLAND *et al.*, 1996) is also depicted. The reaction emanating from [Os] to higher temperatures is the KFMASH reaction: $Grt + Crd + Kfs + Qz = Opx + Sil + L$, which does not intersect the FMAS [Qz] point. The dashed curve AB is the calculated position of the breakdown of fully-hydrated Crd in FMASH according to ARANOVICH and BERMAN (1996). Important assemblage fields are distinguished by shading as given in the keys for KFMASH (+ Kfs + Qz + L) and FMAS.

the stability limits of diagnostic mineral assemblages that are recognised in magnesian pelites and related rocks from UHT terrains worldwide, as discussed in detail by HARLEY (1998a) and briefly summarised below and in Fig. 1.

Mineral assemblages in sapphirine-, spinel- and orthopyroxene-sillimanite granulites have formed the key evidence for UHT metamorphism, and petrogenetic grids involving these assemblages in the FeO-MgO-Al₂O₃-SiO₂ (FMAS) (HENSEN, 1971, 1986, 1987; HENSEN and GREEN, 1973; GREW, 1980; BERTRAND *et al.*, 1991) and KFMASH(H) systems (ELLIS *et al.*, 1980; AUDIBERT *et al.*, 1995; CARRINGTON and HARLEY, 1995a, b; HOLLAND *et al.*, 1996) have provided the basis for interpretation of arrested reaction textures in terms of *P-T* 'paths' or histories. HENSEN (1971) presented the theoretical basis for FMAS petrogenetic grids that are still used to delineate UHT assemblages. HENSEN and GREEN (1973), in their seminal studies of garnet-cordierite (Grt + Crd) assemblages, identified a stability field for sapphirine + quartz (Spr + Qz) at temperatures in excess of 1050°C and

also constrained the key assemblage orthopyroxene + sillimanite + quartz (Opx + Sil + Qz) to occur at pressures beyond maximum cordierite stability conditions of 10–11 kbar. More recent experiments (BERTRAND *et al.*, 1991) have confirmed that Spr + Qz is only stable at >1050°C and that the stability of the assemblage Grt + Crd + Sil + Qz can extend to pressures as high as 11 kbars. A “best-fit” FMAS grid based on the studies noted above is presented here in Fig. 1. This is a compromise grid in terms of the pressure position of the main invariant points, and places the spinel-absent invariant point (*i.e.* [Spl]) at *P-T* conditions consistent with the position of the reaction:



as calculated by ARANOVICH and BERMAN (1996) in the FMASH system (10.2–10.5 kbar at 1040–1050°C: see curve AB in Fig. 1). This pressure position is between the limits defined by HENSEN and GREEN (1973) and BERTRAND *et al.* (1991).

Two other features of the FMAS grid in Fig. 1 require comment. Firstly, the [Qz] point at 950°C and 8 kbar is inferred from topological relations (HENSEN, 1971, 1986) and has not yet been determined or verified experimentally. Hence, the minimum temperatures of UHT assemblages such as Spr + Grt + Crd + Sil (HARLEY, 1986) and Spr + Grt + Opx + Crd are not experimentally constrained to only lie above 900°C, and the minimum pressure of Opx + Sil in FMAS is not well-documented. Secondly, the assemblage spinel + quartz (Spl + Qz) becomes stable at *P-T* conditions below and beyond the [Opx] point, making it a likely UHT indicator provided the assemblage can be represented in the FMAS system. Unfortunately, the interpretation of spinel in UHT granulites is usually complicated by the presence of additional components in the spinels (Zn, Cr), the effect of high f_{O_2} (manifested in Fe³⁺ contents) on spinel stability (HENSEN, 1986; POWELL and SANDIFORD, 1988), and the decomposition of original spinels into polyphase aggregates (*e.g.* spinel_{ss}, magnetite_{ss}, hemoilmenite and corundum: SANDIFORD *et al.*, 1987; WATERS, 1991; DASGUPTA *et al.*, 1995).

In hydrous systems with additional K₂O (KFMASH) the phase relations under UHT conditions will be largely controlled by melt-bearing equilibria, and a free H₂O vapour phase will not be present. Experiments on biotite dehydration-melting (CARRINGTON and HARLEY, 1995a) and related studies of osumilite stability relations (AUDIBERT *et al.*, 1995; CARRINGTON and HARLEY, 1995b) indicate that at pressures of greater than 6 kbar the assemblage osumilite + garnet (Os + Grt) is restricted to temperatures of >900°C in KFMASH (see HARLEY 1998a for discussion) and that this assemblage is replaced by the assemblage Opx + Sil + Kfs + Qz at pressures higher than 8–9 kbar. This result has found impressive application in the Napier Complex, where post-peak near-isobaric cooling (IBC) occurred from peak-T pressures that were higher towards the SSW part of the Complex (SHERATON *et al.*, 1980; HARLEY, 1985; HARLEY and HENSEN, 1990). As discussed by AUDIBERT *et al.* (1995) and CARRINGTON and HARLEY (1995b), this previously-inferred pressure gradient is consistent with the occurrence of Os + Grt in the Tula Mountains and more northerly parts of the UHT region, compared with the more common occurrence of Opx + Sil + Kfs + Qz southwards.

KFMASH reaction grids involving melt (CARRINGTON and HARLEY, 1995a; HOLLAND *et al.*, 1996) also constrain other mineral assemblages formed in the temperature range 875 to 975°C, the lower end of the UHT field (Fig. 1). In the KFMASH ‘simple’ system,

where biotite is not stabilised by additional components (e.g. Ti, F: MOURI *et al.*, 1996), Opx+Sil+Qz assemblages are restricted to pressures greater than 7.5 kbar, and to temperatures greater than 900°C if melting has taken place in the magnesian rock compositions that can access these reactions (e.g. Long Point/Mather Peninsula: HARLEY and FITZSIMONS, 1991; Forefinger Point: HARLEY *et al.*, 1990; Palni Hills: RAITH *et al.*, 1997). Although not explicitly considered in the Qz-present KFMASH grid, Qz-absent assemblages in magnesian rock compositions are also to some extent constrained by the topology presented by CARRINGTON and HARLEY (1995a). In particular, the assemblage Grt+Opx+Sil is restricted to high pressures (>7.5 kbar) and temperatures of >900°C in magnesian migmatitic rocks. Hence, Grt+Opx+Sil assemblages that contain garnets with X_{Mg} in the range 50–70 and orthopyroxene that is highly aluminous (7–11 wt% Al_2O_3 : HARLEY, 1998a) are also good indicators of UHT conditions, a point that is important given their occurrence in a number of UHT terrains and the fact that they are also amenable to conventional thermobarometric analysis. In contrast, melting at lower pressures results in Grt+Crd assemblages that are not diagnostic of UHT conditions. Similarly, melting of Fe-rich rock compositions will only result in the production of garnet-bearing assemblages, which are not diagnostic of UHT conditions.

In summary, FMAS and KFMASH assemblage grids provide a useful framework within which the conditions and histories of UHT metamorphic occurrences can be evaluated. They also provide an independent set of simple constraints with which the results of thermobarometry can be validly compared.

3. Occurrence of UHT Terranes and Localities: GTB Database

An extensive description and assessment of the worldwide occurrence of UHT metamorphism in regional terrains and relatively isolated localities within otherwise lower-grade terrains is presented in HARLEY (1998a). In this work, data on coexisting garnet and orthopyroxene from relatively magnesian pelites and aluminous rocks from several UHT regional metamorphic terrains and localities (88 Grt-Opx pairs) are used to further elucidate the temperature regime. Data compiled for this analysis has been derived from the Napier Complex of Antarctica (SHERATON *et al.*, 1980, 1987; ELLIS *et al.*, 1980; GREW, 1980; HARLEY, 1985; SANDIFORD, 1985); Wilson Lake, Labrador (ARIMA *et al.*, 1986; CURRIE and GITTINS, 1988); the Eastern Ghats of India (LAL *et al.*, 1987; DASGUPTA, 1995); the In Ouzzal complex of Algeria (BERTRAND *et al.*, 1992; OUZEGANE and BOUMAZA, 1996); the Labwor Hills of Uganda (SANDIFORD *et al.*, 1987); the Limpopo Belt (DROOP, 1989); and the Sutam Block of the Aldan Shield, Siberia (MARAKUSHEV and KUDRYAVTSEV, 1965; PERCHUK *et al.*, 1985). Several relatively isolated localities that also preserve evidence for assemblage and *P-T* histories under UHT conditions (e.g. KARSAKOV, 1973; LUTTS and KOPANEVA, 1968; HERD *et al.*, 1986; HARLEY *et al.*, 1990; KRIEGSMAN, 1991; HARLEY, 1998b; MOTOYOSHI and ISHIKAWA, 1997; DAWSON *et al.*, 1997) provide further data that is used in the garnet-orthopyroxene geothermometry evaluation. The Napier Complex and one of the more isolated localities, Mather Peninsula in the Rauer Islands (HARLEY, 1998b), will be examined in more detail with respect to the thermal history evidence that can be extracted from Al_2O_3 zoning in aluminous orthopyroxene.

In the Archaean Napier Complex UHT metamorphic conditions have been defined

from the occurrence of Spr+Opx+Qz, Grt+Opx+Sil+Qz, Spl+Qz and Os+Grt (SHERATON *et al.*, 1980, 1987; ELLIS, 1980; ELLIS *et al.*, 1980; GREW, 1980; HARLEY, 1985; SANDIFORD, 1985; HARLEY and HENSEN, 1990) as well as other indicators such as Mg-rich inverted pigeonite and sub-calcic pyroxenes (SANDIFORD and POWELL, 1986; HARLEY, 1987). As noted in the section on grids and assemblage constraints, post-peak near-isobaric cooling (IBC) occurred at less than 8 kbar in the northern parts of the UHT region and at 9–11 kbar in areas further south (SHERATON *et al.*, 1980; HARLEY, 1985; HARLEY and HENSEN, 1990). The peak-*T* pressure gradient is consistent with Spr+Qz being rimmed by coronas of Crd, Sil and Grt in the Tula Mountains instead of Opx+Sil, which are present in the areas south of Amundsen Bay (SHERATON *et al.*, 1980; MOTOYOSHI and MATSUEDA, 1984; HARLEY, 1985; SANDIFORD, 1985).

The garnet-orthopyroxene data set for the Napier Complex is based on 33 samples from across the UHT area. An important feature of this data is that it spans a broad compositional spectrum in terms of garnet X_{Mg} as well as minor components (*e.g.* grossular contents) compared with the Grt-Opx UHT data available from other areas. Although half the Napier data set involves garnet with $X_{Mg}=50-60$, 10 samples contain garnets with X_{Mg} values in the range 25–45. High alumina contents (8–11 wt% Al_2O_3) are recorded in orthopyroxenes ($X_{Mg}=71-78$) coexisting with the more magnesian garnets, but lower Al_2O_3 contents (4–5 wt%) occur in orthopyroxene coexisting with the less magnesian, higher-grossular garnets ($X_{Mg}=28-40$; $X_{Grs}=5-8$ mol%). The range of preserved compositions provides a useful test for any sensitivity of the geothermometry applied here to real compositional variations.

Other terrains or areas that appear to preserve IBC post-peak histories include Lace (DAWSON *et al.*, 1997), the Labwor Hills (SANDIFORD *et al.*, 1987) and Sipiwesik Lake (ARIMA and BARNETT, 1984). The range in Grt-Opx compositions in samples from these sites is limited (garnet $X_{Mg}=53-63$; orthopyroxene $Al_2O_3=8-10$ wt%), and rather similar to mineral compositions to be summarised below for the numerous sites that preserve apparent or real ITD post-peak histories.

Apart from the extensive data from the Napier Complex, UHT terrains or localities that preserve post-peak ITD or ITD-dominated histories dominate the data set used herein. These include various localities or areas designated as 'ITD cases' in Figs. 2, 3 and 4, which comprise samples from the Eastern Ghats (LAL *et al.*, 1987; DASGUPTA, 1995; DASGUPTA *et al.*, 1994, 1995; SENGUPTA *et al.*, 1990), In Ouzzal (OUZEGANE and BOUMAZA, 1996), St Maurice (HERD *et al.*, 1986), Gruf (DROOP and BUCHER-NURMINEN, 1984), Sri Lanka (KRIEGSMAN, 1991), the Limpopo Belt (DROOP, 1989), and Wilson Lake (ARIMA *et al.*, 1986; CURRIE and GITTINS, 1988). Localities designated separately in Figs. 2, 3 and 4 are Rundvågshetta in Lützow-Holm Bay (MOTOYOSHI and ISHIKAWA, 1997), Forefinger Point in Enderby Land (HARLEY *et al.*, 1990; MOTOYOSHI *et al.*, 1994), and Mather Peninsula (HARLEY and FITZSIMONS, 1991; HARLEY, 1998b). In most of these cases it is not clear whether the ITD is a real 'path' or merely the result of overprinting of an earlier higher-*P* event by an unrelated lower-*P* one, but an analysis of this problem is beyond the scope of the present thermometric evaluation.

A feature common to all these "ITD" occurrences is the presence of Grt+Opx+Sil assemblages, with or without additional quartz, that preserve extensive reaction textures involving the breakdown of initial Mg-rich garnets to symplectites involving Spr, Opx, Crd,

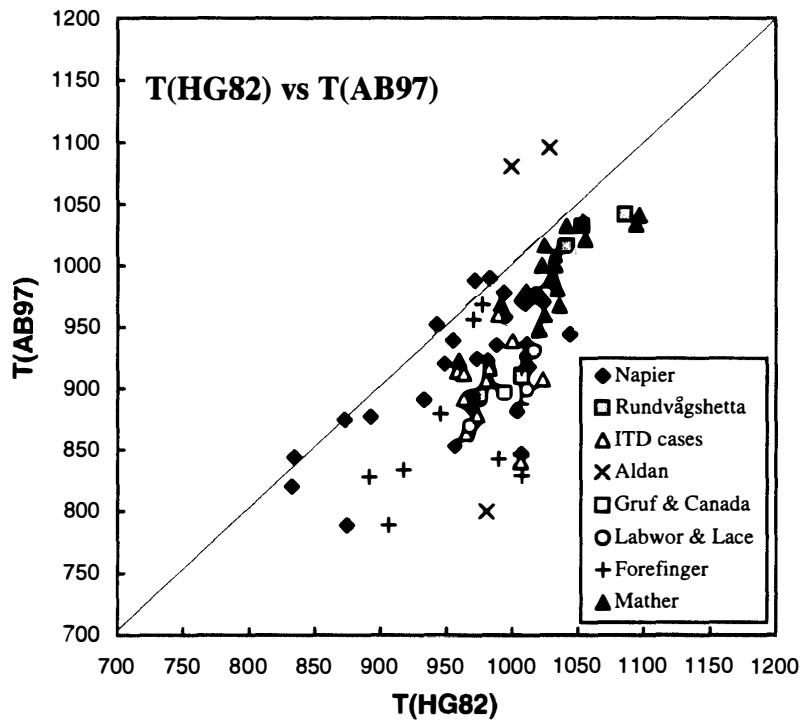
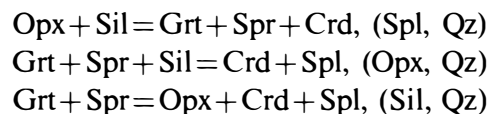


Fig. 2. Temperature diagram (in °C) comparing estimates for UHT terrains and localities as derived from the Al-thermometers developed by HARLEY and GREEN (1982) [$T(HG82)$] and ARANOVICH and BERMAN (1997) [$T(AB97)$]. Diagonal line is the line of equal estimate via each method. The Grt-Op_x data set used in this comparison is split into subsets denoted by different symbols as listed in the key.

Sil and Spl. Such textures, and those that involve replacement of initial Opx+Sil by Spr+Crd coronas, have been interpreted in terms of ITD from P - T conditions near or to higher pressures than the [Spl] point in FMAS. The texturally-deduced ITD paths traverse down-pressure across divariant fields (HENSEN, 1986, 1987, 1988) bounded by reactions such as:



and have usually been interpreted as passing to lower- T than the [Opx] point but higher- T than the [Qz] point in FMAS (e.g. HARLEY *et al.*, 1990; HARLEY, 1998a, b). This ITD evolution therefore takes place over a pressure interval from 11 to *ca.* 8 kbar at 950–1000°C. An important consequence of this type of path for geothermometry is that much of the rock evolution has taken place at temperatures within the UHT field, and if the ITD took place rapidly then there are good prospects for geothermometers being able to locally record those UHT conditions. Although the prograde parts of the P - T histories of most of the ITD areas or localities are poorly known, the presence of kyanite inclusions (Rundvågshetta, Lützow-Holm Bay, Antarctica: MOTOYOSHI and ISHIKAWA, 1997), or possible sillimanite pseudomorphs after kyanite inclusions in magnesian garnet (Palni Hills: RAITH *et al.*, 1997), suggest a clockwise P - T evolution for at least some of these

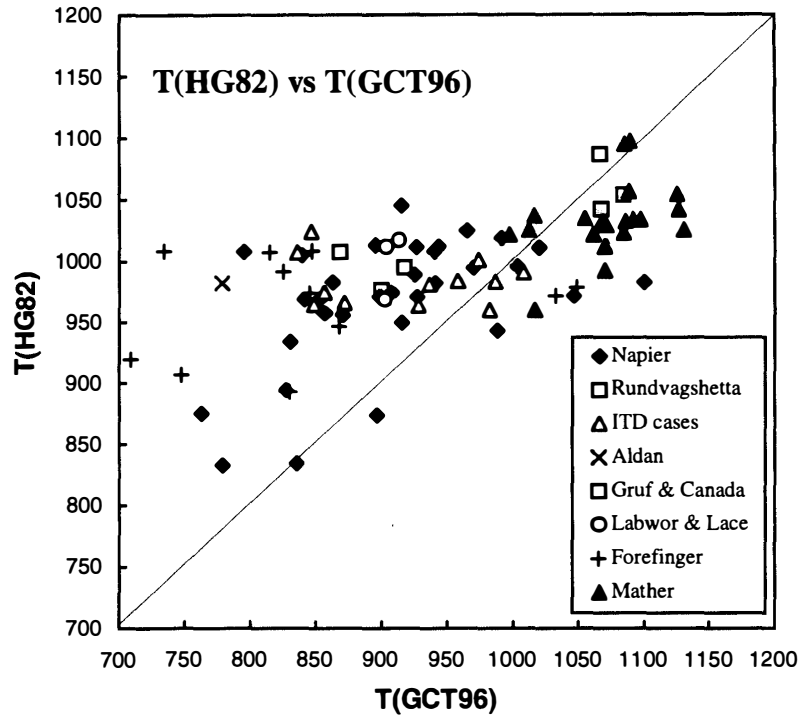


Fig. 3. Temperature diagram (in °C) comparing estimates for UHT terrains and localities as derived from the Al-thermometer developed by HARLEY and GREEN (1982) [$T(HG82)$] and the Fe-Mg Grt-Opx partitioning thermometer of GANGULY *et al.* (1996) [$T(GCT96)$]. Diagonal line is the line of equal estimate via each method. The Grt-Opx data set used in this comparison is split into subsets denoted by different symbols as listed in the key.

UHT areas.

A further similarity between many of these ITD case studies lies in the restricted ranges in the compositions of garnet and orthopyroxene in the assemblages used for thermobarometric calculations. Most of the Grt+Opx+Sil samples used in this compilation contain garnets with X_{Mg} values in the range 50–60 (e.g. northern Eastern Ghats: DASGUPTA *et al.*, 1995; Forefinger Point: HARLEY *et al.*, 1990). There are also several examples in which the garnet X_{Mg} values are greater than 60 ($X_{Mg}=60$ –68: HERD *et al.*, 1986; DROOP and BUCHER-NURMINEN, 1984; HARLEY and FITZSIMONS, 1991; KRIEGSMAN, 1991; RAITH *et al.*, 1997), and at Mather Peninsula (HARLEY and FITZSIMONS, 1991; HARLEY, 1998b) garnet in a Grt+Opx+Sil assemblage retains X_{Mg} values of 68–71. Orthopyroxenes coexisting with garnet in these cases generally retain X_{Mg} values in the range 74–80, and also preserve high Al_2O_3 contents that are typically in the range 7–10 wt% (e.g. MOHAN *et al.*, 1986; HARLEY *et al.*, 1990; RAITH *et al.*, 1997).

4. Thermobarometry Calculations

Many Fe-Mg exchange thermometers, though extensively applied, suffer from post-peak diffusional exchange (HARLEY, 1984; FROST and CHACKO, 1989) that may lead to both mismatch and feedback between temperature and pressure estimates (HARLEY, 1989; FITZSIMONS and HARLEY, 1994). On the other hand, application of retrieval calculations

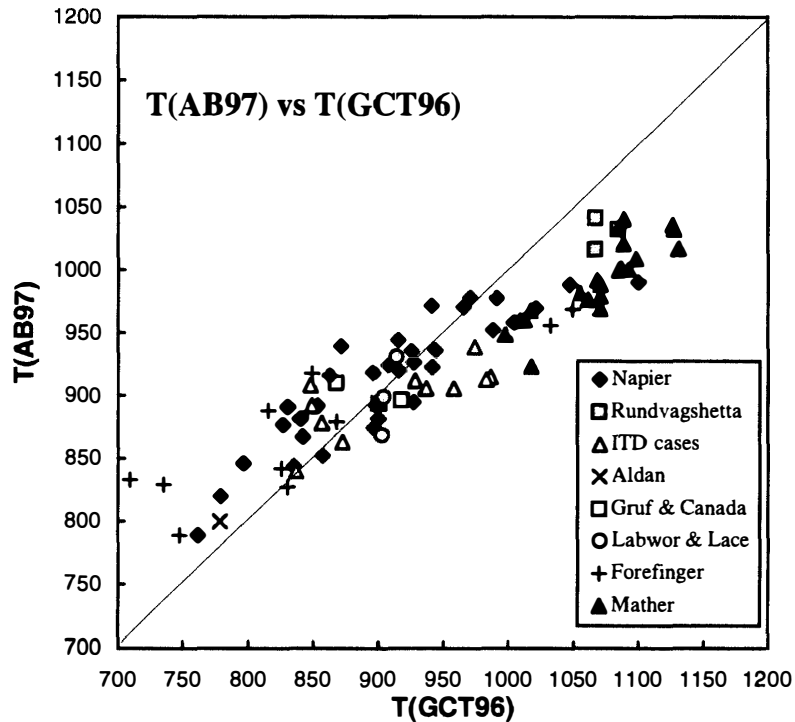


Fig. 4. Temperature diagram (in °C) comparing estimates for UHT terrains and localities as derived from the Al-thermometer developed by ARANOVICH and BERMAN (1997) [$T(AB97)$] and the Fe-Mg Grt-Opx partitioning thermometer of GANGULY *et al.* (1996) [$T(GCT96)$]. Diagonal line is the line of equal estimate via each method. The Grt-Opx data set used in this comparison is split into subsets denoted by different symbols as listed in the key.

(FITZSIMONS and HARLEY, 1994) to several UHT terranes supports the view that a high content of Al_2O_3 in orthopyroxene (8–12 wt%) is one of the most reliable indicators of high metamorphic temperatures (HENSEN, 1987; HARLEY, 1989, 1998a; ARANOVICH and BERMAN, 1997). Hence, thermometers based on the Al_2O_3 contents of orthopyroxene coexisting with garnet, or indeed other aluminous phases, potentially provide the most powerful complementary constraints to the petrogenetic grids for the definition of peak and near-peak temperatures in UHT metamorphism. Two thermometers based on the Al_2O_3 contents of orthopyroxene coexisting with garnet are now available, that of HARLEY and GREEN (1982) [$T(HG82)$] and a new calibration by ARANOVICH and BERMAN (1997) [$T(AB97)$]. In the following discussion these two thermometers are compared using the data set described above, and both are then compared with the most recent thermometric calibration of the exchange of Fe and Mg between garnet and orthopyroxene, that of GANGULY *et al.* (1996) [$T(GCT96)$].

A comparison of the Al-thermometers is presented in Fig. 2. The HARLEY and GREEN (1982) method consistently yields temperature estimates that are similar to or higher than those calculated using ARANOVICH and BERMAN (1997). Average temperatures calculated using all the data, irrespective of locality or source, are $T(HG82) = 990 \pm 49^\circ C$ compared with $T(AB97) = 931 \pm 66^\circ C$. When the data are selected using the filter of only including those Grt-Opx pairs that yield GANGULY *et al.* (1996) temperatures $> 900^\circ C$,

$T(\text{HG82})$ is $1005 \pm 39^\circ\text{C}$ compared with $T(\text{AB97})$ of $962 \pm 51^\circ\text{C}$. From this it is apparent that the thermometer developed by ARANOVICH and BERMAN (1997) is more sensitive to post-peak Fe-Mg exchange (*i.e.* feedback effects) than the simple HARLEY and GREEN (1982) method: the spread in calculated temperature is greater and the average shifts to higher temperatures by *ca.* 30°C when the data is selected to partially account for Fe-Mg exchange. Nevertheless, for most of the Grt-Opx pairs there is quite good agreement (*i.e.* within 50°C) between the two thermometers and both demonstrate that UHT conditions have prevailed in the terrains and localities considered.

It has been noted above that the Grt-Opx data from the Napier Complex span a broad range in X_{Mg} . This data set can therefore be used to assess any effects of X_{Mg} on calculated temperatures. Although both thermometers yield a wide range of temperatures for the Napier Complex and Forefinger Point data ($T(\text{HG82})$: $1045\text{--}833^\circ\text{C}$; $T(\text{AB97})$: $977\text{--}789^\circ\text{C}$), these temperatures are not correlated simply with X_{Mg} in the garnet or orthopyroxene: high temperatures are calculated irrespective of mineral X_{Mg} in both cases.

Two unusual samples from the Aldan Shield yield very high $T(\text{AB97})$ temperatures ($=1081\text{--}1096^\circ\text{C}$) compared with $T(\text{HG82})$ ($=1000\text{--}1029^\circ\text{C}$). This result again arises because the ARANOVICH and BERMAN (1997) thermometer is somewhat sensitive to Fe-Mg exchange, and for these samples the Fe-Mg thermometer ($T(\text{GCT96})$; GANGULY *et al.*, 1996) yields unreasonably high temperatures (see below). Apart from these data, the highest temperature conditions recorded using the Al-thermometry are from two of the ITD localities, Rundvågshetta in Lützow-Holm Bay (MOTOYOSHI and ISHIKAWA, 1997) and Mather Peninsula (HARLEY, 1998b), which both yield maximum temperatures near 1050°C . The average peak temperatures calculated for the Mather Peninsula magnesian assemblages are $T(\text{HG82})=1033 \pm 30^\circ\text{C}$ and $T(\text{AB97})=994 \pm 31^\circ\text{C}$. Notwithstanding any effects of Fe^{3+} in the orthopyroxenes, which would decrease the temperatures calculated by decreasing the amount of Al_2O_3 attributed to MgTs, it is clear that the Al-thermometers have been able to record the UHT conditions that affected these rocks in these cases. Other ITD cases yield lower temperatures (Fig. 2), probably because of more significant post-peak exchange involving Fe-Mg and perhaps Al, but still preserve thermometric evidence for their UHT history.

The 'old' thermobarometer of HARLEY and GREEN (1982) is compared with GANGULY *et al.* (1996) [$T(\text{GCT96})$] in Fig. 3. This plot excludes two Grt-Opx pairs from the Aldan Shield which yield unreasonably high GANGULY *et al.* (1996) temperatures of $>1280^\circ\text{C}$ and hence are considered to have not coexisted in Fe-Mg equilibrium. These samples are the two that also yield anomalously high ARANOVICH and BERMAN (1997) temperatures compared with the less Fe-Mg sensitive HARLEY and GREEN (1982) thermometer. Three main features emerge from this comparison. Firstly, $T(\text{HG82})$ is uniformly high and similar for all but a few samples from the Napier Complex that also yield low $T(\text{GCT96})$; there is no positive correlation between the thermometers. Secondly, $T(\text{GCT96})$ in some cases (*e.g.* Mather Peninsula; Rundvågshetta) exceeds $T(\text{HG82})$ by $50\text{--}100^\circ\text{C}$. Thirdly, the very wide range in $T(\text{GCT96})$ from $1130\text{--}720^\circ\text{C}$ makes its use as a reliable thermometer for UHT metamorphism very uncertain for individual samples: it must be applied with caution and to sets of demonstrably isofacial samples that preferably span a range in bulk composition. The average temperature calculated for the whole data set using GANGULY *et al.* (1996) is $952 \pm 118^\circ\text{C}$, which lies within the UHT field but has

high uncertainty. This average is also biased by the Mather Peninsula data ($T(\text{GCT96}) = 1073 \pm 38^\circ\text{C}$), and if that is excluded then all other UHT terrains yield an average $T(\text{GCT96})$ of $917 \pm 110^\circ\text{C}$, some 75°C less than the average $T(\text{HG82})$ for the same data. Overall, these results support the view that Al is more robust to post-peak exchange than Fe-Mg in most instances of UHT metamorphism.

The thermometer of ARANOVICH and BERMAN (1997) is compared with that of GANGULY *et al.* (1996) in Fig. 4, again with the two Aldan samples excluded from the plot. As would be deduced from the discussion above $T(\text{GCT96})$ is in many cases higher than $T(\text{AB97})$, and by up to 100°C at the highest temperatures. The most noticeable feature of the data array is that there is a positive correlation between $T(\text{AB97})$ and $T(\text{GCT96})$, and though the temperature spread obtained using the Al-thermometer $T(\text{AB97})$ is less than that calculated from the Fe-Mg thermometer it is still sensitive to

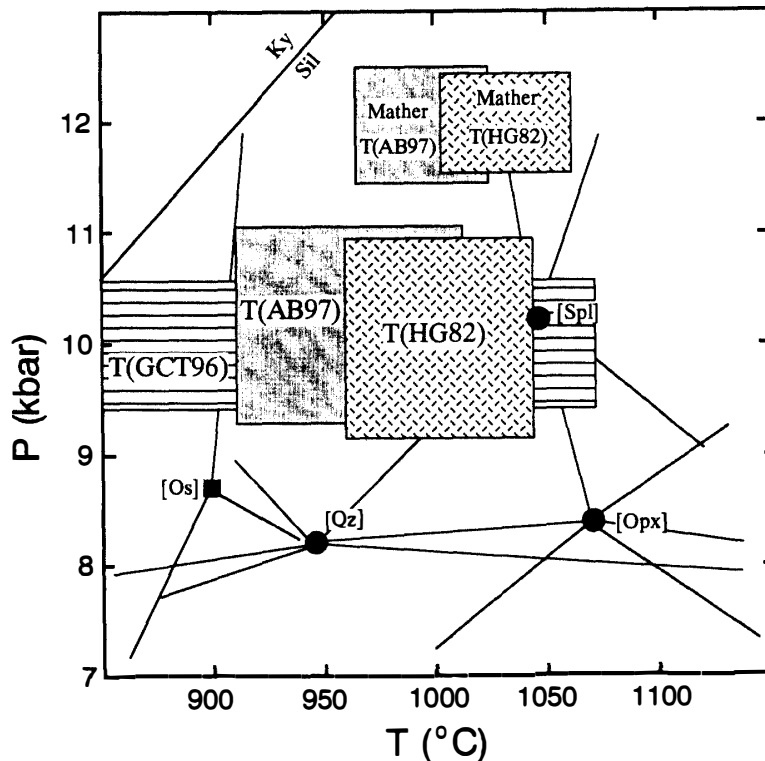


Fig. 5. Pressure-temperature diagram incorporating the thermometric data presented in Figs. 2, 3 and 4 (large shaded boxes), overlain on the assemblage fields of Fig. 1. The size of the large P-T boxes in terms of pressure are schematic, whereas the size of the boxes in terms of temperature are based on the mean and standard deviation for each method. For $T(\text{HG82})$ and $T(\text{AB97})$ the means have been calculated incorporating only those data for which $T(\text{GCT96}) > 900^\circ\text{C}$; for $T(\text{GCT96})$ only the upper part (i.e. from 850°C) of the whole T range is shown. Temperature estimates provided by the Al-thermometers (HARLEY and GREEN, 1982; ARANOVICH and BERMAN, 1997) are in reasonable agreement with the assemblage fields for selected terrains or localities, but average $30\text{--}70^\circ\text{C}$ lower than minimum temperature conditions suggested by the position of the [Spl] point when all data are considered together. Smaller shaded P-T boxes show the estimates via $T(\text{AB97})$ and $T(\text{HG82})$ at 12 kbar for the magnesian UHT gneisses of Mather Peninsula.

Fe-Mg reequilibration. This is reflected in the average temperatures, which are similar for both thermometers if all data are included in the averaging, but with $T(\text{GCT96})$ being slightly higher and less precise (*ie.* $952 \pm 118^\circ\text{C}$ versus $931 \pm 66^\circ\text{C}$). If the Mather Peninsula data are excluded from the GANGULY *et al.* (1996) data analysis the resultant average $T(\text{GCT96})$ is still imprecise but becomes lower than the average $T(\text{AB97})$ calculated from the data set (*ie.* $917 \pm 110^\circ\text{C}$ versus $931 \pm 66^\circ\text{C}$). Overall, this analysis demonstrates that application of the ARANOVICH and BERMAN (1997) thermometer to UHT Grt-Opx assemblages can be enhanced by testing the assemblages for the effects of Fe-Mg exchange using the GANGULY *et al.* (1996) thermometer. Converged temperature estimates could in principle be produced following procedures similar to those developed by FITZSIMONS and HARLEY (1994) and PATTISON and BEGIN (1994) based on back-calculating Grt-Opx Fe-Mg compositions.

In summary, thermometry based on the Al_2O_3 contents of orthopyroxene coexisting with garnet is found to yield temperatures that confirm UHT conditions for most of the terrains and localities considered in this study. The range of this thermometric data is depicted along with the broad assemblage constraint in Fig. 5. As the method of HARLEY and GREEN (1982) is not sensitive to Fe-Mg exchange it provides a robust, though not necessarily accurate, thermometer. Although this thermometer is consistent with assemblage constraints (Fig. 5) it overestimates temperatures by $30\text{--}50^\circ\text{C}$ compared with the Al-thermometer of ARANOVICH and BERMAN (1997). Application of the latter thermometer to estimate peak conditions will in general require testing of and correction for the effects of post-peak Fe-Mg exchange as monitored by thermometers such as GANGULY *et al.* (1996), but the judicious combined use of both Al-thermometer calibrations is likely to further improve estimates of the temperature field of UHT crustal metamorphism.

5. PT Path Interpretation from Al Zoning

The utility of Al_2O_3 in orthopyroxene for estimation of temperatures and elucidation of changes in temperature has also been demonstrated using contoured P - T assemblage grids. The steep dP/dT slopes of Al_2O_3 isopleths in orthopyroxene in assemblages such as Grt+Opx+Sil+Qz and Grt+Opx+Crd+Qz (ARANOVICH and BERMAN, 1996; HARLEY, 1998b) confirm that high equilibrium Al_2O_3 contents in Opx (*e.g.* $>7\text{--}8$ wt%) are simple but robust indicators of UHT conditions in a variety of relevant mineral assemblages. Although discrepancies between the various data sets and approaches to calculating such isopleths lead to differences in the precise wt% Al_2O_3 at a given temperature (*e.g.* ARANOVICH and BERMAN (1996): Al_2O_3 (Opx) = $6\text{--}7$ wt% at $900\text{--}950^\circ\text{C}$; Fig. 6), the sensitivity of Al_2O_3 in orthopyroxene to *changes* in temperature is similar in all studies conducted thus far, rendering it a very useful indicator of heating and cooling if Al_2O_3 zoning is preserved in orthopyroxene. Two contrasting examples of Al_2O_3 zoning in orthopyroxene formed under UHT conditions are briefly described below and used to assess the possible thermal histories of their respective terrains. In the first case the orthopyroxene coexists with garnet and appears to show rimward increases in Al_2O_3 , whereas in the second example the orthopyroxene coexists with sapphirine and quartz and exhibits rimward decreases in Al_2O_3 .

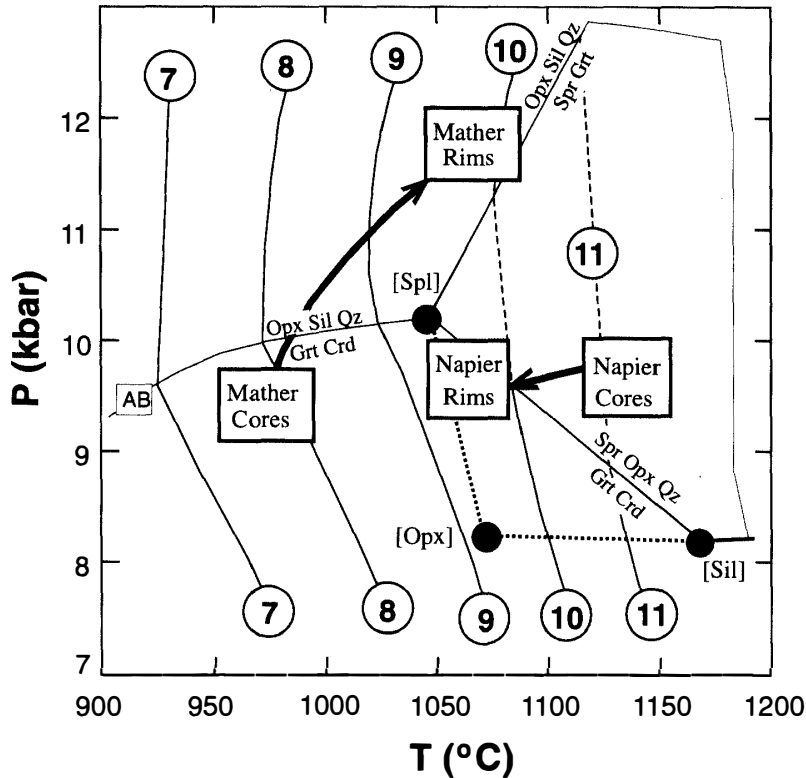


Fig. 6. Pressure-temperature diagram depicting the isopleths of Al_2O_3 in orthopyroxene in the FMAS assemblages $Grt + Crd + Opx + Qz$ and $Grt + Opx + Sil + Qz$ (solid lines; ARANOVICH and BERMAN, 1996) and in the assemblage $Grt + Spr + Opx + Qz$ (long dashed lines, interpolated). Numerals in circles are Al_2O_3 in orthopyroxene (wt%). Bounding FMAS univariants and invariant points (shaded circles) are adapted from HENSEN and GREEN (1973) and BERTRAND et al. (1991) apart from the curve AB, which represents the upper stability of $Grt + Crd$ from ARANOVICH and BERMAN (1996). Shaded field is that of the $Grt + Spr + Opx + Qz$ assemblage. Note the extent of temperature separation (30–40°C) between Al_2O_3 isopleths in the three divariant fields. For each of these fields, and for related sub-assemblages such as $Grt + Opx + Sil$ (Mather Peninsula) or $Spr + Opx + Qz$ (Napier Complex), the steep isopleths require that extensive changes in Opx Al_2O_3 can only occur on heating or cooling. P-T boxes for cores and rims refer to orthopyroxene in the Mather Peninsula (Mather) and R iser Larsen (Napier) assemblages. Absolute temperatures are approximate.

5.1. Mather Peninsula: Zoned orthopyroxene with garnet

The first example of the preservation of Al_2O_3 zoning in orthopyroxene is provided by the magnesian gneisses from Mather Peninsula (Long Point) in the Rauer Islands of East Antarctica. The experimental petrogenetic grid of CARRINGTON and HARLEY (1995a) isoplethed for X_{Mg} ratios of garnet and orthopyroxene (HARLEY, 1998a) indicates that partial melting to produce these Grt ($X_{Mg} > 58$) + $Opx + Sil$ migmatites proceeded at minimum P-T conditions of 8.6 kbar and 910°C. As the peak P-T conditions recorded in these gneisses are 12 kbar and 1050°C or greater, it is considered likely that prograde heating and melting occurred along a near-isobaric or shallow positive dP/dT path, from ca. 900°C up to 1050°C (HARLEY, 1998b).

This model can be evaluated using zoning patterns in orthopyroxenes coexisting with

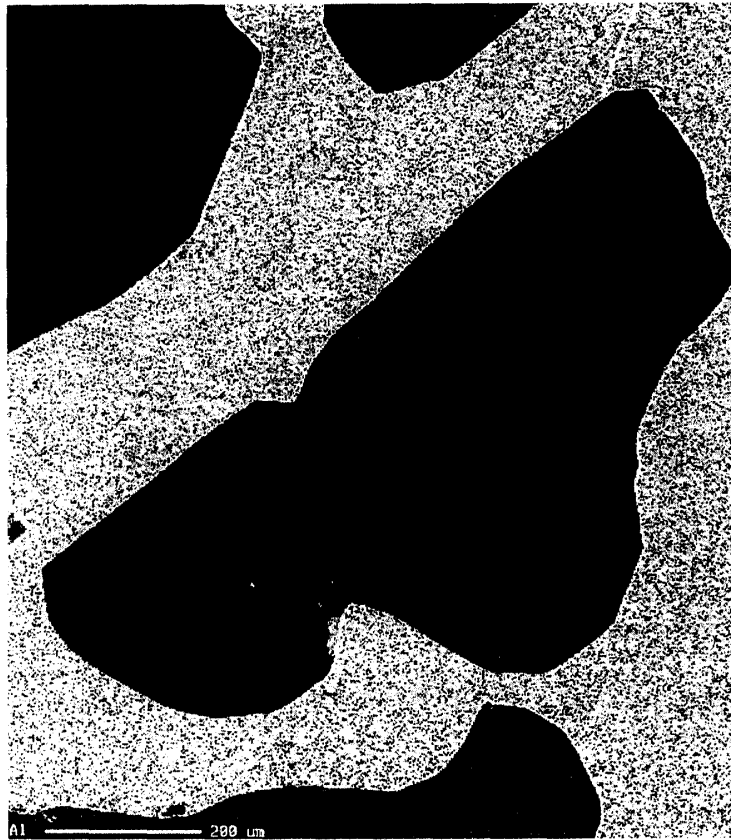


Fig. 7. Colour elemental map of Al in orthopyroxene included in and intergrown with garnet in a Grt + Opx + Sil migmatite sample from Mather Peninsula. Dark blue corresponds to ca. 8 wt% Al_2O_3 , pale blue to > 10 wt% Al_2O_3 in the orthopyroxene; garnet appears as a yellow colour. Negligible Fe-Mg zoning occurs in the garnet, and orthopyroxene only preserves an increase in X_{Mg} within 20–30 of its boundary with garnet (see HARLEY, 1998b for details).

garnet porphyroblasts in quartz-deficient samples. HARLEY (1998b) has described the garnet-orthopyroxene textures in some detail, but further explanation is warranted here in order to provide context for the elemental map presented in Fig. 7. In the Mather Grt + Opx + Sil rocks both garnet and orthopyroxene occur as coarse porphyroblasts, occasionally with coarse sillimanite. On their mutual grain boundaries both garnet and orthopyroxene occur included in or coarsely intergrown with each other, and they form lobate grain arrays of orthopyroxene in garnet or, more rarely, garnet networks in orthopyroxene. These features are consistent with the phases growing simultaneously and interfering as the separate porphyroblasts coarsen. Similarly, a lack of reaction features such as coronas, symplectites and re-entrant grain boundaries between garnet and the lobate orthopyroxene suggests their mutual growth and coexistence under the UHT conditions that prevailed prior to the phase of post-peak ITD that affected Mather Peninsula (HARLEY, 1998b).

The orthopyroxene grains in garnet ($X_{Mg}=66$) are broadly homogeneous in X_{Mg} (=80–82: HARLEY, 1998b) but preserve marked Al_2O_3 zoning that is concentric with grain boundaries. Remarkably, Al_2O_3 increases towards garnet contacts, from 8.0 ± 0.4 wt% in orthopyroxene grain cores to 10.1 ± 0.5 wt% at rims with adjacent garnet. Elemental

mapping of several orthopyroxenes and textural domains demonstrates that this increase in Al_2O_3 occurs in isolated orthopyroxene grains included in garnet, in orthopyroxene adjacent to interlobate garnet, and in all individual orthopyroxene grains or areas occurring within garnet-orthopyroxene interlobate textures. The colour image of Fig. 7 illustrates the concentric geometry of the Al zoning and the excellent equilibrium grain boundaries preserved between the phases. On the basis of these observations HARLEY (1998b) has interpreted the Al zoning as a form of growth zoning, developed as garnet and orthopyroxene have coarsened and grown with each other during heating and melt production at the expense of early biotite and probably sillimanite. On the other hand, the spatial restriction of any Fe-Mg zoning in the orthopyroxenes to very narrow zones on Opx-Grt grain boundaries is attributed to post-peak exchange overprinted on peak- or near-peak Fe-Mg equilibration. The average Fe-Mg temperature calculated using compositional data for the Grt-Opx pair in Fig. 7 is $950 \pm 50^\circ\text{C}$ based on GANGULY *et al.* (1996). This is consistent with UHT Fe-Mg equilibration having occurred and hence implies decoupling of Fe-Mg and Al intragranular diffusion in this case.

The contoured FMAS grid of ARANOVICH and BERMAN (1996) (*e.g.* Fig. 6) can be applied to the Al_2O_3 zoning data in the Mather orthopyroxenes provided it is recognised that only changes in temperature can be deduced because of the absence of quartz from the Grt+Opx+Sil assemblage. Nevertheless, the change in Al_2O_3 of approximately 2.1 ± 0.5 wt% would correspond to an increase in temperature of *ca.* $100 \pm 25^\circ\text{C}$ using this method. This estimate is in reasonable agreement with explicit calculations of the temperatures relevant to orthopyroxene cores and rims or grain-boundaries from Al-thermometry. HARLEY and GREEN (1982) yields core temperatures (at 9 kbar) of 920°C and rims in the range $1030\text{--}1070^\circ\text{C}$ (at 10–12 kbar), giving a core-rim temperature difference of $110\text{--}150^\circ\text{C}$. The Al-thermometer of ARANOVICH and BERMAN (1997), which as discussed above is to some extent affected by Fe-Mg reequilibration, yields lower temperatures (cores 880°C , rims 970°C) but still suggests heating through 90°C if the Al_2O_3 zoning in orthopyroxene was all developed in the presence of garnet.

The interpretation that the Al_2O_3 zoning is a record of heating is strongly dependent on the textural interpretation that garnet and orthopyroxene grew together and in particular that orthopyroxene does not appear to replace or form at the expense of garnet, prior to the onset of later symplectite-forming reactions. Whilst this interpretation is supported by the equilibrium grain boundary shapes shown in Fig. 7, it is valuable to examine alternative ways in which the zoning could form. If Grt+Opx were forming at the expense of Bt+Sil then the Al_2O_3 isopleths in orthopyroxene have a very steep dP/dT (>200 bar/ $^\circ\text{C}$) and only heating could produce the observed zoning. However, if only Grt+Opx are present in the reacting volume, then the Al_2O_3 zoning will be dictated solely by the net-transfer of Al from garnet to orthopyroxene. In this case it would be possible to increase Al_2O_3 in orthopyroxene by consumption of garnet on decompression through a pressure domain at pressures greater than those at which the garnet would decompose to symplectite assemblages (*e.g.* Opx+Sil+Spr or Opx+Spr+Crd). Calculations using HARLEY and GREEN (1982) and ARANOVICH and BERMAN (1997) indicate that UHT-ITD through 2–3 kbar from 14–15 kbar at $1000\text{--}1050^\circ\text{C}$ could lead to the observed increase in Al_2O_3 in orthopyroxene. This would be accomplished by an approximate 10 modal% decrease in garnet within the Grt-Opx areas, which should be reflected in the presence of

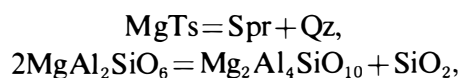
resorbed or resorbed/annealed garnet grain edges. The highest-pressure conditions calculated in this model are within the stability field of kyanite. Sillimanite is the only aluminosilicate polymorph so far recognised from Mather Peninsula, but kyanite or pseudomorphs after it are being searched for in order to discriminate between the heating and decompression models outlined above.

5.2. Napier Complex: Zoned orthopyroxene with sapphirine and quartz

Clockwise (ELLIS, 1987; HARLEY, 1989) and counter-clockwise (MOTOYOSHI and HENSEN, 1989; HENSEN and MOTOYOSHI, 1992) trajectories have been proposed for the prograde path of the UHT granulites in the Napier Complex. In particular, MOTOYOSHI and MATSUEDA (1984) and MOTOYOSHI and HENSEN (1989) have described classic Spr+Qz (+minor Opx) graphic and lamellar intergrowths (see also ELLIS *et al.*, 1980; SHERATON *et al.*, 1987) and interpreted them as pseudomorphs after cordierite, produced during a counter-clockwise *P-T* evolution at *ca.* 1000–1050°C. This insightful textural interpretation warrants further evaluation using a larger range of samples and careful analysis of Spr+Qz assemblages themselves. Some new results from a detailed analysis of mineral composition relationships in a Spr+Opx+Qz assemblage from the Napier Complex (HARLEY and MOTOYOSHI, 1998) are summarized here in order to demonstrate the potential record of extremely high temperature conditions that may be extracted from such rocks.

New evidence that suggests cooling from UHT conditions well beyond the (Spl, Sil) univariant of Fig. 1 (*i.e.* at >1050–1100°C) is seen in Spr+Opx+Qz gneisses from Mt Riiser Larsen in the Tula Mountains, where pressures of 8 kbar have previously been estimated (HARLEY and HENSEN, 1990). Layers containing orthopyroxene and sapphirine porphyroblasts trace out isoclinal folds, but the orthopyroxene and sapphirine have then been recrystallised to granoblastic Spr+Opx+Qz fabrics after this folding. A third textural generation of Spr+Qz is present as intergrown lamellae on and between coarse and polygonal orthopyroxene grains. Hence, the textural history has all occurred within the stability field of Spr+Qz.

Detailed analysis of the porphyroblastic orthopyroxene in this sample shows that its cores contain 11–12.5 wt% Al₂O₃ (average 12.2 wt%). In contrast, porphyroblast rims, recrystallized zones, and orthopyroxene in Opx+Spr+Qtz granoblastic mosaics contain only 8.5–10 wt% (average 9.6 wt%) Al₂O₃. All orthopyroxenes have similar *X*_{Mg} values (82.5). The quantitative analyses are well complemented and amplified by elemental maps for Al, Fe, Mg in this sample. Figure 8 presents colour elemental maps obtained at NIPR, Japan, using the JEOL JXA-8800M electron microprobe. Fe-Mg compositional variations are minor, whereas Al decreases markedly near rims and also along zones parallel to the orthopyroxene cleavage, along which fine Spr+Qz may occur. The continuous reaction;



which progresses from left to right on cooling within the Spr+Opx+Qz field, is considered responsible for the observed textures and Al₂O₃ zoning (HARLEY and MOTOYOSHI, 1999). Analysis of relevant MAS system experiments (ANASTASIOU and SEIFERT, 1972; CHATTERJEE

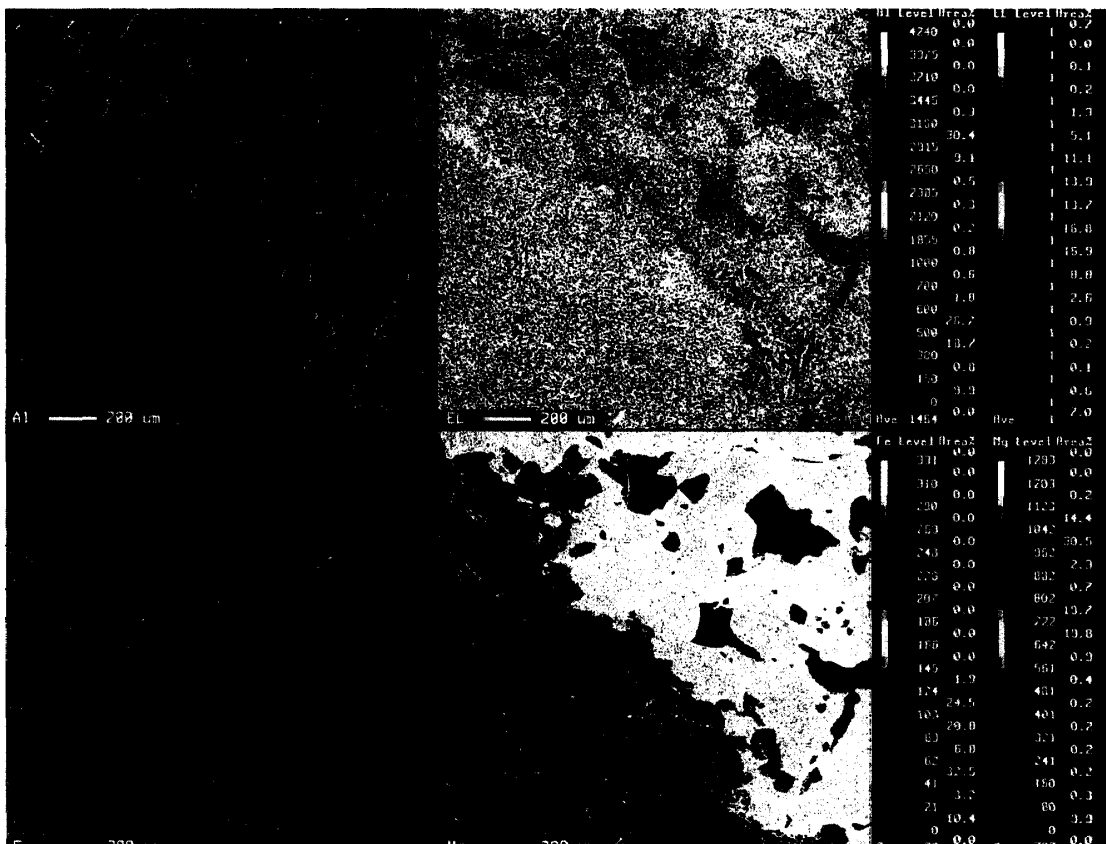


Fig. 8. Colour elemental maps of Al, Fe, Mg and X_{Mg} (denoted as EL) in an orthopyroxene porphyroblast and adjacent sapphirine in a sample from Mount R user Larsen in the Napier Complex (HARLEY and MOTOYOSHI, 1999). For the Al map, dark blue corresponds to ca. 9 wt% Al_2O_3 , pale blue to > 11.5 wt% Al_2O_3 in the orthopyroxene; sapphirine appears as a red colour. Negligible Fe-Mg zoning is present in the orthopyroxene, but concentric increases in X_{Mg} (=3–4 units in X_{Mg}) occur in the polygonal sapphirine (map EL: yellow to red colour change). Note that the decreases in Al_2O_3 (change to dark blue) occur towards and at polygonal orthopyroxene rims and also along linear zones (parallel to cleavage) within the porphyroblast. Sapphirine occurs in higher modal abundance as a granoblastic phase with $Opx + Qz$ than it does as a porphyroblast phase, and in this field of view dominates the granoblastic-textured area.

and SCHREYER, 1972; ARIMA and ONUMA, 1977) by HARLEY and MOTOYOSHI (1999) indicates that isopleths of Al_2O_3 in orthopyroxene coexisting with $Spr + Qz$ are very steeply negative (–140 to –180 bars/ $^{\circ}C$), increase with increasing temperature, and are separated by ca. 20–30 $^{\circ}C$ per 1 wt% Al_2O_3 . A calculated entropy change of -75 ± 15 J/K/mol for this reaction at 1000–1300 $^{\circ}C$, when combined with thermodynamic data for MgTs and Qz from HOLLAND and POWELL (1990), leads to a calculated entropy for sapphirine (S_{Spr}) at 1000 K that is markedly less than the existing published values and hence suggests that further experiments must be carried out on equilibria involving sapphirine (HARLEY and MOTOYOSHI, 1999).

Adopting the parameters obtained from the MAS system and using appropriate mineral a-X relationships, the change in Al_2O_3 in orthopyroxene measured in the Napier

Complex Spr+Opx+Qz assemblage is calculated to result from near-isobaric cooling through at least 80°C (HARLEY and MOTOYOSHI, 1999). Hence, if the minimum temperature for this assemblage is 1040°C then the maximum temperatures in the Napier Complex could have been as high as 1120°C at 8–9 kbars. It is not possible to generate the marked Al₂O₃ zoning through either an increase or decrease in pressure subsequent to the thermal peak: the zoning in this particular assemblage can only be generated through cooling. In addition, the textural history described above indicates that intense deformation either was synchronous with or punctuated this cooling.

As a result of these observations and calculations, any prograde path now proposed for the Napier Complex has to be able to generate temperatures as high as 1120°C at 8–9 kbars and pre-date the deformation and recovery associated with formation of granulitic sapphirine + quartz assemblages. For example, the counter-clockwise *P-T* history proposed by MOTOYOSHI and HENSEN (1989) on the basis of Spr+Qz intergrowths would require revision as such intergrowths would have to have formed from precursor cordierite at significantly higher temperatures than previously thought. An alternative interpretation of the intergrowths described by MOTOYOSHI and HENSEN (1989) is that they too may result from the breakdown of aluminous orthopyroxene rather than cordierite. Whatever the case, it is apparent that further textural and modal studies of these and related UHT intergrowths in the Napier Complex will make an important contribution to any improved definition of the peak and near-peak history.

The Spr+Opx+Qz textural relations described above have thus far only been positively identified from the Napier Complex. However, similar features may occur elsewhere and should be searched for. For example, in the In Ouzzal UHT terrain, OUZEGANE and BOUMAZA (1996) report Spr+Qz replacing Opx+Sil assemblages, and have interpreted this texture in terms of decompression (accompanied by some heating) initially at temperatures greater than those of the [Spl] point. However, this texture may instead reflect the replacement of aluminous orthopyroxene itself by Spr+Qz, as in the Napier Complex (B. HENSEN, pers. comm. 1997). In this case, as shown above, the Spr+Qz could simply reflect cooling from high temperatures within the Spr+Opx+Qz field. This cooling would precede the ITD documented by OUZEGANE and BOUMAZA (1996) from textures involving the breakdown of garnet and Opx+Sil assemblages. Hence, it is important that the orthopyroxenes in the In Ouzzal rock are analysed and mapped to test for any Al zoning that may correlate with Spr+Qz development.

6. Concluding Remarks

I have demonstrated that there is significant and consistent evidence for UHT crustal metamorphism, and that many of its key features can be constrained using present quantitative and semi-quantitative methods. However, to further refine the characterisation of UHT crustal metamorphism more experimental and petrological data and observations are required. For example, reliable experimental data on MAS- and FMAS-system sapphirine are urgently needed to enable the upgrading of internally-consistent thermodynamic data sets and their application to UHT assemblages. Evidence of pre-peak evolutions -the prograde paths- have to be searched for intensively, with a focus on inclusions in porphyroblasts (*e.g.* Ky, Fe-rich Crd) to complement the systematic analysis

and mapping of orthopyroxene for records of Al zoning.

Acknowledgments

I thank the organisers of the 'Origin and Evolution of Continents' meeting in Tokyo for their generous invitation to present aspects of my work on UHT metamorphism. This work has benefitted from discussions over the years with many people, but most notably Bas HENSEN, Ian FITZSIMONS, Mike BROWN, Yoichi MOTOYOSHI, LeonYa ARANOVICH and Mike SANDIFORD. Fieldwork at Long Point (Mather Peninsula) was funded by NERC grant GR9/271 and ASAC projects DV/05/88 and 497. This work was supported by NERC grant GR9/02628 and is a contribution to the granulites theme of IGCP project 368 "Proterozoic Events in East Gondwana". M. ARIMA is thanked for his kind review.

References

- ANASTASIOU, P. and SEIFERT, F. (1972): Solid solubility of Al_2O_3 in enstatite at high temperatures and 1–5 kbar water pressure. *Contrib. Mineral. Petrol.*, **34**, 272–287.
- ARANOVICH, L.Y. and BERMAN, R.G. (1996): Optimized standard state and solution properties of minerals II. Comparisons, predictions, and applications. *Contrib. Mineral. Petrol.*, **126**, 25–37.
- ARANOVICH, L.Y. and BERMAN, R.G. (1997): A new garnet-orthopyroxene thermometer based on reversed Al_2O_3 solubility in $\text{FeO-Al}_2\text{O}_3\text{-SiO}_2$ orthopyroxene. *Am. Mineral.*, **82**, 345–353.
- ARIMA, M. and BARNETT, R.L. (1984): Sapphirine bearing granulites from the Sipiwesk Lake area of the late Archaean Pikwitonei granulite terrain, Manitoba, Canada. *Contrib. Mineral. Petrol.*, **88**, 102–112.
- ARIMA, M., KERRICH, R. and THOMAS, A. (1986): Sapphirine-bearing paragneiss from the northern Grenville province in Labrador, Canada: protolith composition and metamorphic *P-T* conditions. *Geology*, **14**, 844–847.
- ARIMA, M. and ONUMA, K. (1977): The solubility of alumina in enstatite and the phase equilibria in the join $\text{MgSiO}_3\text{-MgAl}_2\text{SiO}_6$ at 10–25 kbar. *Contrib. Mineral. Petrol.*, **61**, 251–265.
- AUDIBERT, N., HENSEN, B.J. and BERTRAND, P. (1995): Experimental study of phase relations involving osumilite in the system $\text{K}_2\text{O-FeO-MgO-Al}_2\text{O}_3\text{-SiO}_2\text{-H}_2\text{O}$ at high pressure and temperature. *J. Metamorph. Geol.*, **13**, 331–344.
- BERTRAND, Ph., ELLIS, D.J. and GREEN, D.H. (1991): The stability of sapphirine-quartz and hypersthene-sillimanite-quartz assemblages: An experimental investigation in the system $\text{FeO-MgO-Al}_2\text{O}_3\text{-SiO}_2$ under H_2O and CO_2 conditions. *Contrib. Mineral. Petrol.*, **108**, 55–71.
- BERTRAND, Ph., OUZEGANE, Kh. and KIENAST, J.-R. (1992): *P-T-X* relationships in the Precambrian Al-Mg-rich granulites from In Ouzzal, Hoggar, Algeria. *J. Metamorph. Geol.*, **10**, 17–31.
- BOHLEN, S.R. (1991): On the formation of granulites. *J. Metamorph. Geol.*, **9**, 223–229.
- CARRINGTON, D.P. and HARLEY, S.L. (1995a): Partial melting and phase relations in high-grade metapelites: an experimental petrogenetic grid in the KFMASH system. *Contrib. Mineral. Petrol.*, **120**, 270–291.
- CARRINGTON, D.P. and HARLEY, S.L. (1995b): The stability of osumilite in metapelitic granulites. *J. Metamorph. Geol.*, **13**, 613–625.
- CHATTERJEE, N.D. and SCHREYER, W. (1972): The reaction $\text{enstatite}_{\text{ss}} + \text{sillimanite} = \text{sapphirine}_{\text{ss}} + \text{quartz}$ in the system $\text{MgO-Al}_2\text{O}_3\text{-SiO}_2$. *Contrib. Mineral. Petrol.*, **36**, 49–62.
- CURRIE, K.L. and GITTINS, J. (1988): Contrasting sapphirine parageneses from Wilson Lake, Labrador and their tectonic implications. *J. Metamorph. Geol.*, **6**, 603–622.
- DASGUPTA, S. (1995): Pressure-temperature evolutionary history of the Eastern Ghats granulite province:

- recent advances and some thoughts. *India and Antarctica During the Precambrian*. Mem. Geol. Soc. India, **34**, 101–110.
- DASGUPTA, S., SANYAL, S., SENGUPTA, P. and FUKUOKA, M. (1994): Petrology of granulites from Anakapalle-evidence for Proterozoic decompression in the Eastern Ghats, India. *J. Petrol.*, **35**, 433–459.
- DASGUPTA, S., SENGUPTA, P., EHL, J., RAITH, M. and BARDHAN, S. (1995): Reaction textures in a suite of spinel granulites from the Eastern Ghats Belt, India: Evidence for polymetamorphism, a partial petrogenetic grid in the system KFMASH and the roles of ZnO and Fe₂O₃. *J. Petrol.*, **36**, 435–461.
- DAWSON, J.B., HARLEY, S.L., RUDNICK, R.L. and IRELAND, T. (1997): Equilibration and reaction in Archaean sapphirine granulite xenoliths from the Lace kimberlite pipe, South Africa. *J. Metamorph. Geol.*, **15**, 253–266.
- DROOP, G.T.R. (1989): Reaction history of garnet-sapphirine granulites and conditions of Archaean high-pressure granulite facies metamorphism in the Central Limpopo Mobile Belt, Zimbabwe. *J. Metamorph. Geol.*, **7**, 383–403.
- DROOP, G.T.R. and BUCHER-NURMINEN, K. (1984): Reaction textures and metamorphic evolution of sapphirine-bearing granulites from the Gruf Complex, Italian Central Alps. *J. Petrol.*, **25**, 766–803.
- ELLIS, D.J. (1980): Osumilite-sapphirine-quartz granulites from Enderby Land, Antarctica: *P-T* conditions of metamorphism, implications for garnet-cordierite equilibria and the evolution of the deep crust. *Contrib. Mineral. Petrol.*, **74**, 201–210.
- ELLIS, D.J. (1987): Origin and evolution of granulites in normal and thickened crust. *Geology*, **15**, 167–170.
- ELLIS, D.J., SHERATON, J.W., ENGLAND, R.N. and DALLWITZ, W.B. (1980): Osumilite-sapphirine-quartz granulites from Enderby Land, Antarctica-mineral assemblages and reactions. *Contrib. Mineral. Petrol.*, **72**, 123–143.
- FITZSIMONS, I.C.W. and HARLEY, S.L. (1994): The influence of retrograde cation exchange on granulite *P-T* estimates and a convergence technique for the recovery of peak metamorphic conditions. *J. Petrol.*, **35**, 543–576.
- FROST, B.R. and CHACKO, T. (1989): The granulite uncertainty principle: limitations on thermobarometry in granulites. *J. Geol.*, **97**, 435–450.
- GANGULY, J., CHENG, W. and TIRONE, M. (1996): Thermodynamics of aluminosilicate garnet solid solution: new experimental data, an optimized model, and thermodynamic applications. *Contrib. Mineral. Petrol.*, **126**, 137–151.
- GREW, E.S. (1980): Sapphirine+quartz association from Archaean rocks in Enderby Land, Antarctica. *Am. Mineral.*, **65**, 821–836.
- HARLEY, S.L. (1984): An experimental study of the partitioning of Fe and Mg between garnet and orthopyroxene. *Contrib. Mineral. Petrol.*, **86**, 359–373.
- HARLEY, S.L. (1985): Garnet-orthopyroxene bearing granulites from Enderby Land, Antarctica: Metamorphic pressure-temperature-time evolution of the Archaean Napier Complex. *J. Petrol.*, **26**, 819–856.
- HARLEY, S.L. (1986): A sapphirine-cordierite-garnet-sillimanite granulite from Enderby Land, Antarctica: Implications for FMAS petrogenetic grids in the granulite facies. *Contrib. Mineral. Petrol.*, **94**, 452–460.
- HARLEY, S.L. (1987): A pyroxene-bearing metaironstone and other pyroxene-granulites from Tonagh Island, Enderby Land, Antarctica: Further evidence for very high temperature (>980°C) Archaean regional metamorphism in the Napier Complex. *J. Metamorph. Geol.*, **5**, 341–356.
- HARLEY, S.L. (1989): The origins of granulites: A metamorphic perspective. *Geol. Mag.*, **126**, 215–247.
- HARLEY, S.L. (1998a): On the occurrences and characterisation of Ultrahigh-Temperature (UHT) Crustal Metamorphism. *What Drives Metamorphism and Metamorphic Reactions?*, ed. by P.J. TRELOAR and P.J. O'BRIEN. Bath, Geological Society, 81–107 (Geol. Soc. London, Spec.

- Publ., **138**).
- HARLEY, S.L. (1998b): Ultrahigh temperature granulite metamorphism (1050°C, 12 kbar) and decompression in garnet (Mg70)-orthopyroxene-sillimanite gneisses from the Rauer Group, East Antarctica. *J. Metamorph. Geol.*, **16**, 541-562.
- HARLEY, S.L. and FITZSIMONS, I.C.W. (1991): Pressure-temperature evolution of metapelitic granulites in a polymetamorphic terrane: The Rauer Group, East Antarctica. *J. Metamorph. Geol.*, **9**, 231-243.
- HARLEY, S.L. and GREEN, D.H. (1982): Garnet-orthopyroxene barometry for granulites and peridotites. *Nature*, **300**, 697-701.
- HARLEY, S.L. and HENSEN, B.J. (1990): Archaean and Proterozoic high-grade terranes of East Antarctica (40-80°E): a case study of diversity in granulite facies metamorphism. High-temperature Metamorphism and Crustal Anatexis, ed. by J.R. ASHWORTH and M. BROWN. London, Unwin Hyman, 320-370.
- HARLEY, S.L. and MOTOYOSHI, Y. (1999): Al-zoning in orthopyroxene in a sapphirine quartzite: Evidence for >1120°C UHT metamorphism in the Napier Complex, Enderby Land, Antarctica. to be published in *Contrib. Mineral. Petrol.*
- HARLEY, S.L., HENSEN, B.J. and SHERATON, J.W. (1990): Two-stage decompression in orthopyroxene-sillimanite granulites from Forefinger Point, Enderby Land, Antarctica: Implications for the evolution of the Archaean Napier Complex. *J. Metamorph. Geol.*, **8**, 591-613.
- HENSEN, B.J. (1971): Theoretical phase relations involving cordierite and garnet in the system MgO-FeO-Al₂O₃-SiO₂. *Contrib. Mineral. Petrol.*, **33**, 191-214.
- HENSEN, B.J. (1986): Theoretical phase relations involving garnet and cordierite revisited: The influence of oxygen fugacity on the stability of sapphirine and spinel in the system Mg-Fe-Al-Si-O. *Contrib. Mineral. Petrol.*, **92**, 191-214.
- HENSEN, B.J. (1987): *P-T* grids for silica-undersaturated granulites in the systems MAS (*n*+4) and FMAS (*n*+3)-tools for the derivation of *P-T* paths of metamorphism. *J. Metamorph. Geol.*, **5**, 255-271.
- HENSEN, B.J. (1988): Chemical potential diagrams and chemographic projections: application to sapphirine-granulites from Kiranur and Ganguvarpatti, Tamil Nadu. Evidence for rapid uplift in part of the South Indian Shield? *Neues Jahrb. Mineral. Abh.*, **158**, 193-210.
- HENSEN, B.J. and GREEN, D.H. (1973): Experimental study of the stability of cordierite and garnet in pelitic compositions at high pressures and temperatures. III. Synthesis of experimental data and geological applications. *Contrib. Mineral. Petrol.*, **38**, 151-166.
- HENSEN, B.J. and MOTOYOSHI, Y. (1992): Osumilite-producing reactions in high-temperature granulites from the Napier Complex, East Antarctica: tectonic implications. *Recent Progress in Antarctic Earth Science*, ed. by Y. YOSHIDA *et al.* Tokyo, Terra Sci. Publ., 87-92.
- HERD, R.K., ACKERMAN, D., WINDLEY, B.F. and RONDOT, J. (1986): Sapphirine-garnet rocks, St. Maurice area, Quebec: Petrology and implications for tectonics and metamorphism. *The Grenville Province*, ed. by J.M. MOORE *et al.*, Spec. Pap. Geol. Assoc. Canada, **31**, 241-253.
- HOLLAND, T.J.B. and POWELL, R. (1990): An enlarged and updated internally consistent data-set with uncertainties and correlations: The system K₂O-Na₂O-CaO-MgO-MnO-FeO-Fe₂O₃-Al₂O₃-TiO₂-SiO₂-C-H₂-O₂. *J. Metamorph. Geol.*, **8**, 89-124.
- HOLLAND, T.J.B., BABU, E.V.S.S.K. and WATERS, D.J. (1996): Phase relations of osumilite and dehydration melting in pelitic rocks: A simple thermodynamic model for the KFMASH system. *Contrib. Mineral. Petrol.*, **124**, 383-394.
- KARSAKOV, L.P. (1973): Pyrope-bronzite-sillimanite schist of Eastern Stanovik and the pressure-temperature conditions during its metamorphism. *Dokl. Akad. Nauk SSSR*, **210**, 187-190 (translated to *Dokl. Acad. Sci. USSR, Earth Sci. Sect.*, **210**, 171-173, 1973).
- KRIEGSMAN, L. (1991): Sapphirine-bearing granulites from central Sri Lanka: outcrop description and mineral chemistry. *The crystalline crust of Sri Lanka. Part I. Summary of research of the German-Sri Lankan Consortium*, ed. by A. KRÖNER. *Geol. Surv. Dept. Sri Lanka Prof. Paper* **5**, 178-187.

- LAL, R.K., ACKERMAN, D. and UPADHYAY, H. (1987): *P-T-X* relationships deduced from corona textures in sapphirine-spinel-quartz assemblages from Paderu, southern India. *J. Petrol.*, **28**, 1139-1168.
- LUTTS, B.G. and KOPANEVA, L.N. (1968): A pyrope-sapphirine rock from the Anabar Massif and its conditions of metamorphism. *Dokl. Akad. Nauk SSSR*, **179**, 1200-1202 (translated to *Dokl. Acad. Sci. USSR, Earth Sci. Sect.*, **179**, 161-163, 1968).
- MARAKUSHEV, A.A. and KUDRYAVTSEV, V.A. (1965): Hypersthene-sillimanite paragenesis and its implication. *Dokl. Akad. Nauk SSSR*, **164**, 179-182. (translated to *Dokl. Acad. Sci. USSR, Earth Sci. Sect.*, **164**, 145-148, 1966).
- MOHAN, A., ACKERMAN, D. and LAL, R.K. (1986): Reaction textures and *P-T-X* trajectory in the sapphirine-spinel bearing granulites from Ganguvarpatti, Southern India. *Neues Jahrb. Mineral. Abh.*, **154**, 1-19.
- MOTOYOSHI, Y. and HENSEN, B.J. (1989): Sapphirine-quartz-orthopyroxene symplectites after cordierite in the Archaean Napier Complex, Antarctica: Evidence for a counterclockwise *P-T* path? *Eur. J. Mineral.*, **1**, 467-471.
- MOTOYOSHI, Y. and ISHIKAWA, M. (1997): Metamorphic and structural evolution of granulites from Rundvågshetta, Lützow-Holm Bay, East Antarctica. *The Antarctic Region: Geological Evolution and Processes*, ed. by C.A. RICCI. Siena, Terra Antarctica Publications, 65-72.
- MOTOYOSHI, Y. and MATSUEDA, H. (1984): Archaean granulites from Mt. Riiser-Larsen in Enderby Land, East Antarctica. *Mem. Natl. Inst. Polar Res., Spec. Issue*, **33**, 103-125.
- MOTOYOSHI, Y., ISHIKAWA, M. and FRASER, G.L. (1994): Reaction textures in granulites from Forefinger Point, Enderby Land, East Antarctica: An alternative interpretation on the metamorphic evolution of the Rayner Complex. *Proc. NIPR Symp. Antarct. Geosci.*, **7**, 101-114.
- MOURI, H., GUIRAUD, M. and HENSEN, B.J. (1996): Petrology of biotite-sapphirine-bearing Al-Mg granulites from Ihouhaouene, In Ouzal, Hoggar, Algeria: An example of phlogopite stability at high temperature. *J. Metamorph. Geol.*, **14**, 725-738.
- OUZEGANE, K. and BOUMAZA, S. (1996): An example of ultrahigh-temperature metamorphism: orthopyroxene-sillimanite-garnet, sapphirine-quartz and spinel-quartz parageneses in Al-Mg granulites from In Hihaou, In Ouzal, Hoggar. *J. Metamorph. Geol.*, **14**, 693-708.
- PATTISON, D.R.M. and BEGIN, N.J. (1994): Compositional maps of metamorphic orthopyroxene and garnet: evidence for a hierarchy of closure temperatures and implications for geothermometry of granulites. *J. Geol.*, **12**, 387-410.
- PERCHUK, L.L., ARANOVICH, L.Y., PODLESSKII, K.K., LAVRENT'eva, I.V., GERASIMOV, V.Y., KITSUL, V.I., KORSKOV, L.P. and BERDNIKOV, N.V. (1985): Precambrian granulites of the Aldan Shield, eastern Siberia, the USSR. *J. Metamorph. Geol.*, **3**, 265-310.
- POWELL, R. and SANDIFORD, M. (1988): Sapphirine and spinel phase relationships in the system $\text{FeO-MgO-Al}_2\text{O}_3\text{-SiO}_2\text{-TiO}_2\text{-O}_2$ in the presence of quartz and hypersthene. *Contrib. Mineral. Petrol.*, **98**, 64-71.
- RAITH, M., KARMAKAR, S. and BROWN, M. (1997): Ultra-high temperature metamorphism and multistage decompressional evolution of sapphirine granulites from the Palni Hill Ranges, southern India. *J. Metamorph. Geol.*, **15**, 379-400.
- SANDIFORD, M. (1985): The metamorphic evolution of granulites at Fyfe Hills: Implications for Archaean crustal thickness in Enderby Land, Antarctica. *J. Metamorph. Geol.*, **3**, 155-178.
- SANDIFORD, M. and POWELL, R. (1986): Pyroxene exsolution in granulites from Fyfe Hills, Enderby Land, Antarctica: Evidence for 1000°C metamorphic temperatures in Archaean continental crust. *Am. Mineral.*, **71**, 946-954.
- SANDIFORD, M. and POWELL, R. (1991): Some remarks on high-temperature-low pressure metamorphism in convergent orogens. *J. Metamorph. Geol.*, **9**, 333-340.
- SANDIFORD, M., NEALL, F.B. and POWELL, R. (1987): Metamorphic evolution of aluminous granulites from Labwor Hills, Uganda. *Contrib. Mineral. Petrol.*, **95**, 217-225.
- SENGUPTA, P., DASGUPTA, S., BHATTACHARYA, P.K., FUKUOKA, M., CHAKRABORTI, S. and BHOWMICK, S. (1990): Petro-tectonic imprints in the sapphirine granulites from Anantagiri, Eastern Ghats

- mobile belt, India. *J. Petrol.*, **31**, 971-996.
- SHERATON, J.W., OFFE, L.A., TINGEY, R.J. and ELLIS, D.J. (1980): Enderby Land, Antarctica; an unusual Precambrian high-grade metamorphic terrain. *J. Geol. Soc. Aust.*, **27**, 1-18.
- SHERATON, J.W., TINGEY, R.J., BLACK, L.P., OFFE, L.A. and ELLIS, D.J. (1987): Geology of Enderby Land and Western Kemp Land, Antarctica. *Bull. Aust. Bur. Miner. Resour.*, **223**, 51 p.
- WATERS, D.J. (1991): Hercynite-quartz granulites: phase relations, and implications for crustal processes. *Eur. J. Mineral.*, **3**, 367-386.

(Received February 16, 1998; Revised manuscript accepted April 27, 1998)

Appendix table. Garnet-orthopyroxene thermobarometry of UHT occurrences.

Area	X _{Mg}	X _{grs}	X _{Mg}	X _{Al}	P(kb)	K _d	T(H84)	T(HG82)	T(AB97)	T(GCT96)
Napier Cores										
McIntyre 4518	0.594	0.022	0.768	0.150	11	2.26	850	971	894	927
4518	0.584	0.022	0.768	0.150	11	2.36	824	971	882	900
49659	0.530	0.014	0.720	0.190	11	2.28	842	1045	944	916
49607	0.549	0.021	0.774	0.175	11	2.81	728	1007	846	796
49657	0.527	0.015	0.710	0.145	11	2.20	865	982	923	941
Hydrographer 49576	0.571	0.040	0.755	0.163	11	2.32	842	1011	927	927
Charles 3971	0.589	0.025	0.722	0.144	11	1.81	1009	983	990	1101
3970	0.414	0.058	0.630	0.100	11	2.41	825	949	920	916
Hollingsworth 49891	0.523	0.035	0.695	0.175	10	2.08	904	1018	977	992
Debenham 3964	0.528	0.039	0.746	0.155	10	2.63	764	969	867	842
Marsland 3410	0.485	0.019	0.676	0.180	9	2.22	849	989	935	926
3411	0.425	0.034	0.620	0.170	9	2.21	857	1008	971	941
Tonagh 49786	0.542	0.028	0.735	0.215	9	2.34	818	1013	918	896
49817	0.570	0.016	0.765	0.184	9	2.46	786	957	852	857
49809	0.568	0.018	0.723	0.201	9	1.99	922	996	958	1004
49856	0.514	0.016	0.688	0.219	9	2.09	887	1025	970	966
49868	0.535	0.028	0.747	0.211	9	2.57	767	1004	881	841
49831	0.584	0.010	0.730	0.224	9	1.93	941	1011	969	1021
49774	0.555	0.027	0.744	0.182	9	2.33	821	971	892	899
Crohn 3597	0.282	0.076	0.524	0.078	9	2.80	738	894	876	828
Howard Hills 4593	0.470	0.028	0.690	0.165	9	2.51	779	969	891	854
Trail 4833	0.571	0.029	0.744	0.215	9	2.18	862	1012	936	944
Sones 49748	0.294	0.086	0.565	0.064	9	3.12	690	833	820	779
49740	0.456	0.042	0.676	0.190	8	2.49	782	983	915	864
49734	0.405	0.058	0.589	0.128	8	2.11	891	943	952	989
49749	0.376	0.063	0.620	0.131	8	2.71	745	934	891	831
3552	0.489	0.053	0.650	0.165	8	1.94	946	971	988	1047
Riiser-Larsen 3423	0.304	0.050	0.510	0.080	8	2.38	810	873	874	897
49382	0.467	0.029	0.720	0.132	8	2.93	694	875	789	763
Hardy 4549	0.480	0.029	0.678	0.190	8	2.28	828	974	924	908
Ward Rocks 3532	0.433	0.022	0.612	0.190	8	2.07	889	995	978	971
Miller 4085	0.280	0.076	0.510	0.082	6	2.68	744	834	844	835
Wilkinson's Peak 4528	0.370	0.040	0.585	0.198	6	2.40	790	956	939	871
Rundvagshetta	0.595	0.045	0.739	0.207	11	1.93	969	1087	1042	1067
	0.595	0.045	0.739	0.175	11	1.93	969	1042	1016	1067
	0.600	0.050	0.740	0.180	11	1.90	983	1054	1033	1085
In Ouzzal	0.610	0.040	0.770	0.180	10	2.14	886	1001	939	975
Munwatte	0.680	0.030	0.817	0.165	11	2.10	901	983	916	986
Hakurutale	0.640	0.030	0.823	0.205	10	2.62	763	1007	840	837
Anakapalle	0.590	0.030	0.780	0.165	10	2.46	796	966	863	873
St Maurice	0.640	0.040	0.790	0.158	10	2.12	894	959	914	983
Anabar	0.611	0.040	0.821	0.205	9	2.92	705	981	799	779
Stanovoy	0.600	0.025	0.693	0.164	11	1.50	1179	1029	1096	1286
Aldan-Sutam	0.635	0.001	0.711	0.162	11	1.41	1234	1000	1081	1332
In Ouzzal	0.640	0.020	0.790	0.210	9	2.12	879	984	906	959
Gruf	0.610	0.020	0.780	0.190	10	2.27	841	995	896	918
Sipiwesk	0.560	0.030	0.750	0.164	10	2.36	821	976	894	901
Wilson Lake	0.500	0.020	0.710	0.180	10	2.45	796	1008	909	869
Paderu	0.520	0.030	0.710	0.146	10	2.26	847	964	912	928
Ganguvarpatti	0.520	0.020	0.730	0.162	10	2.50	785	974	878	857
Palni	0.600	0.030	0.770	0.172	10	2.23	855	981	906	937
Madugula	0.500	0.030	0.720	0.190	10	2.57	772	1024	907	847
Limpopo	0.450	0.040	0.680	0.136	10	2.60	770	964	891	849

Appendix table. Continued.

Limpopo	0.560	0.030	0.720	0.165	10	2.02	921	991	960	1009
Labwor	0.530	0.020	0.720	0.190	10	2.28	838	1017	931	914
Forefinger Point	0.580	0.030	0.730	0.155	10	1.96	944	971	956	1033
Forefinger Point										
2203	0.502	0.051	0.720	0.132	10	2.55	784	946	879	868
2203	0.449	0.035	0.678	0.164	10	2.58	771	1008	916	848
2203	0.479	0.033	0.704	0.150	10	2.59	770	974	886	846
2209	0.485	0.055	0.726	0.168	10	2.81	734	1007	887	816
2209	0.502	0.047	0.732	0.110	10	2.71	751	893	827	830
2220	0.606	0.048	0.808	0.180	10	2.74	746	991	842	826
2220	0.606	0.044	0.750	0.158	10	1.95	953	978	968	1049
2223	0.496	0.045	0.757	0.123	10	3.17	675	907	789	748
2223	0.494	0.047	0.761	0.182	10	3.26	663	1008	829	735
2231	0.320	0.049	0.620	0.100	10	3.47	638	919	833	709
Lace	0.606	0.026	0.782	0.200	10	2.33	826	1012	899	904
Lace	0.627	0.021	0.796	0.175	10	2.32	827	968	869	903
Mather Peninsula										
	0.710	0.040	0.825	0.170	12	1.93	975	1029	988	1071
	0.710	0.040	0.825	0.160	12	1.93	975	1011	979	1071
	0.710	0.040	0.825	0.150	12	1.93	975	993	969	1071
	0.715	0.046	0.820	0.180	12	1.82	1024	1054	1036	1127
	0.710	0.033	0.820	0.175	12	1.86	998	1034	1000	1093
	0.710	0.060	0.825	0.200	12	1.93	983	1097	1041	1089
	0.710	0.060	0.825	0.175	12	1.93	983	1056	1021	1089
	0.710	0.030	0.813	0.170	12	1.78	1035	1026	1016	1131
	0.700	0.035	0.820	0.175	12	1.95	962	1035	981	1055
	0.695	0.045	0.805	0.170	12	1.81	1025	1042	1032	1128
	0.690	0.025	0.810	0.170	12	1.92	972	1022	976	1061
	0.690	0.036	0.805	0.170	12	1.85	1002	1034	1008	1098
	0.680	0.045	0.815	0.170	12	2.07	923	1037	968	1017
	0.680	0.035	0.800	0.210	12	1.88	990	1095	1033	1085
	0.675	0.030	0.795	0.170	12	1.87	994	1032	1001	1087
	0.670	0.030	0.795	0.170	12	1.91	976	1032	992	1068
	0.660	0.035	0.800	0.165	12	2.06	923	1025	960	1012
	0.660	0.035	0.785	0.160	12	1.88	991	1023	1000	1086
	0.657	0.030	0.800	0.165	12	2.09	912	1021	948	998